

1 **The effects of temperature, salinity, and the carbonate system on**
2 **Mg/Ca in *Globigerinoides ruber* (white): a global sediment trap**
3 **calibration**

4
5 William R Gray^{1*}†, Syee Weldeab¹, David W Lea¹, Yair Rosenthal², Nicolas Gruber³,
6 Barbara Donner⁴, Gerhard Fischer⁴

7 ¹Department of Earth Science/Marine Science Institute, University of California,
8 Santa Barbara, California, USA

9 ²Marine and Coastal Sciences, Rutgers University, New Jersey, USA

10 ³Institute of Biogeochemistry and Pollutant Dynamics, ETH Zürich, Zürich,
11 Switzerland

12 ⁴MARUM, University of Bremen, Bremen, Germany

13

14 *corresponding author: wrg4@st-andrews.ac.uk

15 †Present address: Department of Earth and Environmental Sciences, University of St
16 Andrews, St Andrews, UK

17

18 *Abstract*

19 The Mg/Ca of planktic foraminifera *Globigerinoides ruber* (white) is a widely
20 applied proxy for tropical and sub-tropical sea-surface temperature. The accuracy
21 with which temperature can be reconstructed depends on how accurately relationships
22 between Mg/Ca and temperature and the multiple secondary controls on Mg/Ca are
23 known; however, these relationships remain poorly quantified under oceanic
24 conditions. Here, we present new calibrations based on 440 sediment trap/plankton
25 tow samples from the Atlantic, Pacific and Indian Oceans, including 130 new samples

26 from the Bay of Bengal/Arabian Sea and the tropical Atlantic Ocean. Our results
27 indicate temperature, salinity and the carbonate system all significantly influence
28 Mg/Ca in *G. ruber* (white). We propose two calibration models: The first model
29 assumes pH is the controlling carbonate system parameter. In this model, Mg/Ca has a
30 temperature sensitivity of $6.0 \pm 0.8 \text{ \%}/^\circ\text{C}$ (2σ), a salinity sensitivity of $3.3 \pm 2.2 \text{ \%}/\text{PSU}$
31 and a pH sensitivity of $-8.3 \pm 7.7 \text{ \%}/0.1 \text{ pH units}$; The second model assumes carbonate
32 ion concentration ($[\text{CO}_3^{2-}]$) is the controlling carbonate system parameter. In this
33 model, Mg/Ca has a temperature sensitivity of $6.7 \pm 0.8 \text{ \%}/^\circ\text{C}$, a salinity sensitivity of
34 $5.0 \pm 3.0 \text{ \%}/\text{PSU}$ and a $[\text{CO}_3^{2-}]$ sensitivity of $-0.24 \pm 0.11 \text{ \%}/\mu\text{mol kg}^{-1}$. In both models,
35 the temperature sensitivity is significantly lower than the widely-applied sensitivity of
36 $9.0 \pm 0.6 \text{ \%}/^\circ\text{C}$. Application of our new calibrations to down-core data from the Last
37 Glacial Maximum, considering whole ocean changes in salinity and carbonate
38 chemistry, indicate a cooling of $2.4 \pm 1.6 \text{ }^\circ\text{C}$ in the tropical oceans if pH is the
39 controlling parameter and $1.5 \pm 1.4 \text{ }^\circ\text{C}$ if $[\text{CO}_3^{2-}]$ is the controlling parameter.

40

41 *Keywords:* Mg/Ca; planktic foraminifera; SST; salinity; carbonate chemistry

42

43 **1. Introduction**

44

45 Planktic foraminiferal Mg/Ca paleothermometry is one of the most widely
46 applied techniques to reconstruct sea-surface temperature (SST) (e.g. Lea *et al.*, 2000;
47 Weldeab *et al.*, 2007; Schmidt and Lynch-Stieglitz, 2011; Mohtadi *et al.*, 2014).
48 Fundamental to robust SST reconstruction is accurate knowledge of the relationship
49 between foraminiferal Mg/Ca and temperature, as well as the multiple secondary
50 influences on Mg incorporation into foraminiferal calcite. The substantial biological

51 mediation of Mg incorporation into foraminiferal calcite necessitates species-specific
52 calibrations (Nürnberg, 1996; Rosenthal *et al.*, 1997; Lea *et al.*, 1999; Erez *et al.*,
53 2003).

54

55 *Globigerinoides ruber* (white) is the most widely used species for
56 reconstructing tropical and subtropical SST due to its cosmopolitan nature, high
57 abundance, and shallow habitat depth (0-50 m) (Hemleben *et al.*, 1989; Schiebel and
58 Hemleben, 2017). Estimates of the sensitivity of Mg/Ca in *G. ruber* (w) to
59 temperature fall between 5-10 % per °C (Table 1), and the most widely-applied
60 calibration has a sensitivity of 9.0 ± 0.6 %/°C (2σ) (Dekens *et al.*, 2002; Anand *et al.*,
61 2003). Studies of *G. ruber* (w) grown in laboratory culture, where calcification
62 temperature is well constrained, yield a temperature sensitivity of 8 ± 3 %/°C
63 (Kisakürek *et al.*, 2008).

64

65 Since the early development of Mg/Ca paleothermometry, salinity and
66 carbonate chemistry have been known to exert a secondary influence on Mg/Ca
67 (Nürnberg *et al.* 1996; Lea *et al.*, 1999). Estimates of the sensitivity of Mg/Ca in *G.*
68 *ruber* to salinity vary widely. Laboratory culture studies indicate a salinity sensitivity
69 of 3-5 % per salinity unit (Kisakürek *et al.*, 2008; Hönisch *et al.*, 2013), whereas
70 several core-top studies suggest a significantly higher sensitivity of 15-29 %/PSU
71 (Ferguson *et al.*, 2008; Arbueszowski *et al.* 2010; Mathien-Blard and Bassinot, 2009),
72 although subsequent work has revised down these core-top estimates (Bousetta *et al.*,
73 2011; Hertzberg *et al.*, 2013; Hönisch *et al.*, 2013). More recently, a Bayesian
74 multivariate fit to core-top data suggested a salinity sensitivity of 3.9 ± 1.2 %/PSU
75 (Khider *et al.*, 2015), similar to the results of the culture studies.

76

77 Laboratory culture studies show that the carbonate chemistry of seawater, as
78 expressed by pH or carbonate ion concentration ($[\text{CO}_3^{2-}]$), significantly effects
79 planktic foraminiferal Mg/Ca. Mg/Ca decreases as pH (and $[\text{CO}_3^{2-}]$) increases, with a
80 sensitivity of ~5-10% per 0.1 pH unit (Lea *et al.*, 1999; Russell *et al.*, 2004;
81 Kisakürek *et al.*, 2008; Evans *et al.*, 2016). Despite the significant effect of carbonate
82 chemistry observed within culture studies, the influence of carbonate chemistry on
83 Mg/Ca in planktic foraminifera that have calcified under oceanic conditions (i.e. none
84 laboratory-grown) has not been previously investigated.

85

86 Here, we assess the relationship between Mg/Ca in *G. ruber* (w) and
87 temperature, salinity, and the carbonate system using samples collected by sediment
88 trap and plankton tow. Sediment trap and plankton tow samples minimise the
89 influence of post-depositional calcite dissolution and/or secondary overgrowth
90 deposition that hinder core-top studies, whilst allowing the analysis of foraminifera
91 that have calcified under oceanic conditions within a well constrained time-period.
92 We have generated new data from a transect of sediment traps located along an
93 isotherm with a strong salinity gradient in the Bay of Bengal and Arabian Sea, which
94 we use to assess the effects of salinity. We have also generated new data from a
95 sediment trap in the tropical Atlantic Ocean, off Mauritania; in these samples, we
96 separated foraminifera by morphotype and into narrow size fractions to assess the
97 effects of biological variability on Mg/Ca. Our newly generated data are combined
98 with all previously published *G. ruber* (w) Mg/Ca data from foraminifera collected by
99 sediment trap and plankton tow. We use climatological data to calculate temperature,
100 salinity, pH and $[\text{CO}_3^{2-}]$ at the depth habitat range of *G. ruber* (w) for each of the
101 newly generated and previously published trap/tow samples, and constrain the

102 individual effects of temperature and salinity, pH and $[\text{CO}_3^{2-}]$ on Mg/Ca using subsets
103 of data where covariance between environmental variables is negligible.

104

105 **2. Materials and Methods**

106

107 *2.1 Arabian Sea and Bay of Bengal sediment trap samples*

108 We utilised 51 samples from sediment trap deployments NBBT09 (17.383°N,
109 89.700°E; 1450 m water depth), CBBT06 (11.033°N, 84.433°E; 899 m water depth),
110 SBBT09 (5.400°N, 86.767°E; 886 m water depth), and JGOFS AS02-M5 (10.003 °N,
111 65.005 °E; 2363 m water depth) (Unger *et al.*, 2003; Honjo *et al.*, 1999) (see
112 supplementary material (SM) and Table S1). These sediment trap deployments form a
113 transect spanning a large salinity gradient (~4 units), with ~no change in mean annual
114 temperature between the sites (Fig. 1). Foraminifera were picked from the 200 to 400
115 μm size fraction (see SM), and between 5-30 individuals of *G. ruber* (*w*) *sensu stricto*
116 (Wang [2000]) were used per sample for trace element analysis.

117

118 Foraminifera were cleaned following a modified version of the method of Pak
119 *et al.*, (2004) and the acidified samples were analysed at Rutgers University using
120 magnetic-sector ICP-MS (Thermo Element XR) (SM). Reproducibility of consistency
121 standards with a Mg/Ca similar to *G. ruber* (*w*) was 0.03 mmol/mol (0.6%) (2σ). Six
122 of the foraminiferal samples (~12%) were split into replicates and cleaned/analysed
123 separately, with a reproducibility of 0.12 mmol/mol (2.2%) (2σ). The resulting Mg/Ca
124 data are given in Table S2.

125

126 *2.2 Tropical Atlantic sediment trap samples*

127 We measured Mg/Ca ratios in foraminifera collected by a sediment trap
128 located off Mauritania, in the eastern tropical Atlantic (Fig. 1). The samples were
129 collected in trap deployments CB-7, CB-9, CB-10, CB-12 and CB-13 located at 21.27
130 °N, 20.75 °W between 705-3610 m water depth (Fischer *et al.*, 2016) (SM and Table
131 S1).

132

133 We separated the foraminifera from each trap sample by morphotype (Wang
134 [2000]), and into narrow size fractions to assess the potential impact of morphotype
135 and test size on Mg/Ca, resulting in a total of 79 foraminiferal samples. 15-25
136 individual foraminifera were cleaned following a modified version of the method of
137 Pak *et al.*, (2004) and the acidified samples were analysed by ICP-OES (Perkin
138 Elmer Optima 3300 R) at the University of Bremen (SM and Table S2).
139 Reproducibility of our consistency standard was 0.14 Mg/Ca mmol/mol (~2%)
140 (2σ).

141

142 2.3 Calculating calcification temperature and salinity

143 As the vast majority of sediment trap deployments do not have associated
144 continuous in-situ CTD measurements of temperature and salinity, previous studies
145 have used either $\delta^{18}\text{O}_{\text{calcite-water}}$ or satellite temperatures (see SM). Here, we calculate
146 temperature/salinity at the depth habitat of *G. ruber* (w) for the time-period
147 represented by each trap/tow sample using WOA13 monthly climatologies (Boyer *et al.*
148 *et al.*, 2013) (Fig. 2). We use Monte Carlo simulation to fully propagate the uncertainty
149 in temperature and salinity relating to habitat depth range, error associated with the
150 climatological mean (a combination of short-term and inter-annual variability), and
151 change in temperature/salinity during the sampling period (SM). Following this

152 approach, samples from locations/time-periods with significant temperature and
153 salinity variation within upper water-column or substantial short term and/or inter-
154 annual variability are associated with a wide distribution of temperature and salinity;
155 samples from locations/time-periods with a more homogenous upper water-column or
156 less short term and/or inter-annual variability are associated with a narrower
157 distribution of temperature and salinity. These distributions of temperature and salinity
158 are fully propagated as uncertainty in our regressions (section 2.6). All temperature
159 and salinity values reported are for the 0-50m depth range (Hemleben *et al.*, 1989;
160 Schiebel and Hemleben, 2017), unless otherwise stated. Hydrographic data for all
161 samples are shown on Figure S1 and given in Table S2.

162

163 To test the accuracy of the temperature estimates generated by this approach
164 we used the WOA13 monthly climatological temperature to predict the temperatures
165 at the only trap site with continuous CTD coverage, located within the Sargasso Sea
166 (SM and Fig. S2). The result demonstrates that the differences between the CTD
167 temperatures and climatological temperatures are normally distributed around a mean
168 of ~ 0 ($p > 0.88$) (Fig. S2). Thus, while the use of climatological temperature may
169 result in random error (noise) in the calibration, it does not lead to systematic error
170 (inaccuracy) in the calibration. In section 3.9, we discuss how much of the noise
171 results from the use of climatological temperature.

172

173 *2.4 Estimation of carbonate system parameters*

174 As there is no carbonate chemistry database with a sufficient temporal, spatial
175 and depth resolution to provide carbonate system estimates in the depth habitat of *G.*
176 *ruber* (w), we first generated monthly carbonate system parameter estimates for each

177 trap/tow site throughout the upper water-column. This is achieved by combining the
178 gridded GLODAPv2 dissolved inorganic carbon (DIC) and alkalinity (Alk) data for
179 the interior ocean (Key *et al.*, 2015; Lauvset *et al.*, 2016) with monthly DIC and Alk
180 estimates for the surface ocean, calculated using the monthly $p\text{CO}_2$ climatologies from
181 the Landschützer *et al.* (2014a, b) gridded database and estimates of alkalinity from
182 the algorithms of Lee *et al.*, (2006). Monthly values for DIC and Alk throughout the
183 upper ocean were then obtained by interpolating between the surface value and the
184 seasonally invariant ocean interior value using density. pH and $[\text{CO}_3^{2-}]$ were
185 calculated from DIC and Alk using the OCMIP2 routines (SM).

186

187 To obtain pH and $[\text{CO}_3^{2-}]$ for the time interval represented by each sample at
188 the habitat depth of *G. ruber* (w), the monthly gridded values were interpolated using
189 the method described above for temperature and salinity, with Monte-Carlo
190 simulation to account for the uncertainty in the estimates relating to habitat depth and
191 sampling interval (SM and Fig. 2). All pH and $[\text{CO}_3^{2-}]$ values reported are for the 0-
192 50m depth range, unless otherwise stated. pH and $[\text{CO}_3^{2-}]$ estimates for all samples
193 are shown in Figure S2, and are given in Table S2.

194

195 *2.5 Compilation of sediment trap/plankton tow data*

196 The compilation of previously published data comprises 310 data points from
197 16 sediment trap/plankton tow sites in the Atlantic, Pacific and Indian oceans (Fig. 1,
198 SM and Table S1). All Mg/Ca data, along with the original reference for the Mg/Ca
199 data, size fraction, and morphotype are given in Table S2. When combined, our newly
200 generated Mg/Ca data (130 samples) and the compilation of previously-published
201 data comprise 440 sediment trap/plankton tow samples from 20 sites in Atlantic,

202 Pacific and Indian basins. Within the dataset temperature, salinity, pH (seawater
203 scale) and $[\text{CO}_3^{2-}]$ range from 18.4 to 29.1 °C, 32.6 to 36.7 PSU, 7.99 to 8.12 pH
204 units, and 191 to 252 $\mu\text{mol/kg}$, respectively (Fig. S1). The variation in temperature
205 within the dataset is mainly driven by seasonal variability at each site, whereas the
206 variation in salinity is mainly driven by the location of the sites in differing oceanic
207 regions. Variations in pH and $[\text{CO}_3^{2-}]$ are driven by both seasonal variability and
208 regional differences; this essentially decouples the temperature, salinity and
209 pH/ $[\text{CO}_3^{2-}]$ variation within the dataset; however, there is covariance between
210 temperature and salinity ($r = -0.63$), temperature and pH ($r = -0.68$), salinity and pH ($r =$
211 -0.67), salinity and $[\text{CO}_3^{2-}]$ ($r = -0.52$), and pH and $[\text{CO}_3^{2-}]$ ($r = -0.55$) (Fig. S1).

212

213 *2.6 Regression analysis*

214 We first analyse the global dataset before taking subsets of this dataset to
215 circumvent covariance between predictor variables, and better constrain the
216 sensitivity of Mg/Ca to temperature, salinity and the carbonate system. Coefficients
217 are from linear and non-linear least-squares regression. Confidence intervals are
218 derived from bootstrapping (Efron, 1979), and we account for the uncertainty in
219 predictor variables (T, S, pH, $[\text{CO}_3^{2-}]$) with Monte-Carlo simulation. Following this
220 approach, the uncertainty associated with the T, S, pH and $[\text{CO}_3^{2-}]$ estimate of each
221 sample is fully propagated through to the uncertainty associated with the derived
222 sensitivities. All confidence intervals reported are $\pm 2\sigma$, unless otherwise stated.
223 Additional regression results are given in Table S3.

224

225 **3. Results and Discussion**

226

227 *3.1 Arabian Sea/Bay of Bengal and Tropical Atlantic data*

228 All newly generated Mg/Ca data are shown on Figure 3. Within the Arabian Sea/Bay
229 of Bengal dataset temperature, salinity, pH and $[\text{CO}_3^{2-}]$ range from 26.6 to 29.1 °C,
230 32.58 to 36.49 PSU, 7.99 to 8.05 pH units, and 191 to 246 $\mu\text{mol/kg}$, respectively (Fig.
231 S1); Mg/Ca ranges from 4.68 to 6.67 mmol/mol (Fig. 3). These data are discussed in
232 detail in section 3.4, where we use the data to constrain the effect of salinity on
233 Mg/Ca.

234

235 Within the newly generated tropical Atlantic dataset temperature, salinity, pH
236 and $[\text{CO}_3^{2-}]$ range from 20.4 to 23.7 °C, 36.47 to 36.70 PSU, 8.06 to 8.07 pH units,
237 217 to 232 $\mu\text{mol/kg}$ (Fig. S1); Mg/Ca ranges from 3.00 to 5.57 mmol/mol (Fig. 3).

238

239 3.2 Biological variability

240 Before investigating the environmental controls on Mg/Ca, we first assess the
241 potential influence of morphotype and test size on Mg/Ca. To explore whether there is
242 a significant difference in Mg/Ca between the *sensu stricto* and *sensu lato*
243 morphotypes of *G. ruber* (w) (Wang, 2000) we focus on the newly generated data
244 from the tropical Atlantic, where Mg/Ca was analysed on both the *sensu stricto* and
245 *sensu lato* morphotypes from the same sediment trap cup. A Student's T test shows no
246 significant difference in mean Mg/Ca of the two morphotypes ($p = 0.21$; $n = 32$)
247 (Figure S3). A combined analysis our or newly generated data with previously
248 published data from the Indian Ocean (Mohtadi *et al.*, 2009) demonstrates there is no
249 significant difference in the mean, or variance, of Mg/Ca in the two morphotypes
250 across the Atlantic and Indian basins (Fig. 4a).

251

252 Test size is also known to influence Mg/Ca in *G. ruber* (w) (Friedrich *et al.*,
253 2012). To assess the possible effects of test size we utilise our newly generated
254 dataset from the tropical Atlantic, in which foraminifera were separated into narrow
255 size fractions. While Mg/Ca generally increases with increasing test size, ~33% of the
256 samples do not show an increasing trend with test size (Fig. 4). Overall, there is no
257 significant difference in mean Mg/Ca in the 150 to 425 μm size range, however the
258 variance in the 300-425 μm size fraction is significantly higher than the 150-250 μm
259 size fraction (Fig. S4). Excluding the 33% of data that do not show a Mg/Ca increase
260 with test size, the data appear to fall on similar trend line of $\Delta\text{Mg/Ca}$, with a slope of
261 $0.35 \text{ mmol mol}^{-1}/100 \mu\text{m}$ (Fig. 4e). The samples showing no trend are not related to a
262 particular season or year, and within the same cup sample the *sensu stricto* and *sensu*
263 *lato* morphotypes often show differing trends. Comparing the slope of the relationship
264 between Mg/Ca and test size and the slope of temperature change with depth in the
265 water-column during the interval of time represented by the trap sample shows no
266 significant relationship (Fig. 4f); this likely indicates the relationship between Mg/Ca
267 and test size is not due to changing environmental conditions within the water-column
268 and differing habitat-depths of each size fraction. A recent study suggested that the
269 size of planktic foraminifera may influence the biomineralisation response to
270 changing carbonate chemistry (Henehan *et al.*, 2017). While it is possible that the
271 sensitivity with which Mg/Ca responds to an environmental variable (T, S, pH, $[\text{CO}_3^{2-}$
272]) may also be affected by size, it is not possible to test this hypothesis with the newly
273 generated tropical Atlantic data due to the limited range in environmental variables at
274 this site (Fig. S4). Our results suggest that while test size can clearly influence Mg/Ca,
275 the relationship between test size and Mg/Ca is likely to vary not only temporally at
276 sites (Fig. 4c and 4d), but also between sites, and cannot be systematically corrected

277 for. We will return to test size in section 3.9 in a discussion of potential sources of
278 noise within the calibration.

279

280 3.3 Global calibration

281 When our newly generated Mg/Ca data are combined with all previously
282 published Mg/Ca from sediment traps/plankton tows (section 2.5), Mg/Ca within the
283 dataset ranges from 2.57 to 6.94 mmol/mol and generally increases with temperature
284 (Fig. 5). Regressing Mg/Ca against only temperature results in a temperature
285 sensitivity of $5.3 \pm 0.4 \text{ \%}/^\circ\text{C}$ ($p < 10^{-16}$) (Eq. S1). This is significantly lower than the
286 widely-applied $9.0 \pm 0.6 \text{ \%}/^\circ\text{C}$ sensitivity of the calibration of Dekens *et al.*
287 (2002)/Anand *et al.* (2003) (Fig. 5). Throughout the text, we refer to the ‘multi-
288 species’ equation of Anand *et al.* (2003), as this is by far the most widely applied
289 calibration. Incorporating salinity into the regression model results in a slightly higher
290 temperature sensitivity of $6.2 \pm 0.5 \text{ \%}/^\circ\text{C}$ ($p < 10^{-16}$) and a salinity sensitivity of
291 $3.3 \pm 1.2 \text{ \%}/\text{PSU}$ ($p < 10^{-7}$) (Eq. S2). The slight increase in the temperature sensitivity
292 is due to the negative covariance of temperature and salinity within the dataset.

293

294 Next, we add the carbonate system parameters into the regression model,
295 assuming it is either pH or $[\text{CO}_3^{2-}]$ (and not both) that influences Mg/Ca.
296 Incorporating pH (seawater scale) into the regression model results in a temperature
297 sensitivity of $5.3 \pm 0.6 \text{ \%}/^\circ\text{C}$ ($p < 10^{-16}$), a salinity sensitivity of $4.7 \pm 1.2 \text{ \%}/\text{PSU}$ ($p <$
298 10^{-12}), and a pH sensitivity of $-15.2 \pm 5.4 \text{ \%}/0.1 \text{ pH units}$ ($p < 10^{-9}$) (Eq. S3). The slight
299 change in temperature and salinity sensitivity is due to the covariance of pH with
300 temperature and salinity within the dataset. Substituting $[\text{CO}_3^{2-}]$ for pH results in a
301 temperature sensitivity of $7.5 \pm 0.6 \text{ \%}/^\circ\text{C}$ ($p < 10^{-15}$), a salinity sensitivity of 7.8 ± 1.6

302 %/PSU ($p < 10^{-16}$), and a $[\text{CO}_3^{2-}]$ sensitivity of -0.35 ± 0.12 %/ $\mu\text{mol kg}^{-1}$ ($p < 10^{-9}$) (Eq.
303 S4). Again, the increase in temperature and salinity sensitivities from is due to the
304 covariance of $[\text{CO}_3^{2-}]$ with salinity (and salinity with temperature).

305

306 Several key features stand out from these regressions. Firstly, temperature,
307 salinity and $\text{pH}/[\text{CO}_3^{2-}]$ all have a significant influence on Mg/Ca, with temperature
308 exerting the greatest influence. Secondly, the widely-applied calibration of Dekens *et al.*
309 *al.* (2002) and Anand *et al.* (2003) does not accurately describe the sediment
310 trap/plankton tow data (Fig. 5). Thirdly, the sensitivity of Mg/Ca to salinity is
311 significantly lower than the estimates derived from coretop studies (Ferguson *et al.*,
312 2008; Arbueszowski *et al.*, 2010; Mathien-Blard and Bassinot, 2009). Finally, the
313 covariance between predictor variables (temperature, salinity, pH, $[\text{CO}_3^{2-}]$) is
314 influencing the results of the regressions. In most instances this influence is relatively
315 minor; however, a more significant difference is seen when $[\text{CO}_3^{2-}]$ is incorporated
316 into the regression model.

317

318 In the next three sections, we address the issue of covariance to more
319 accurately constrain the sensitivity of Mg/Ca in *G. ruber* (w) to temperature, salinity,
320 and the carbonate system. To constrain the sensitivity of Mg/Ca to salinity (section
321 3.4) and temperature (section 3.5), we take subsets of the global dataset where
322 covariance between predictor variables is reduced. We test the derived sensitivities
323 from these subsets of data for the influence of covariance by re-running the regression
324 models, each time including in an additional predictor variable; when the inclusion of
325 additional predictor variables does not change the resulting sensitivity, the influence
326 of covariance is demonstrated to be negligible.

327

328 3.4 Sensitivity of Mg/Ca to salinity

329 To assess the sensitivity of Mg/Ca to salinity we focus on our new data from
330 the Arabian Sea and Bay of Bengal. Regressions of the entire Arabian Sea/Bay of
331 Bengal dataset demonstrate that covariance of predictor variables is influencing the
332 results (SM). To better constrain the sensitivity of Mg/Ca to salinity, we take a subset
333 of the Arabian Sea/Bay of Bengal dataset from a more limited temperature range (28
334 to 29 °C; Fig. 3) and exclude two samples with pH <8.00 to reduce the variation in
335 pH ($n = 29$, ~60% of Arabian Sea/Bay of Bengal dataset). We opt for this temperature
336 range as the mean annual temperature at all four sites is ~28.5 °C, thus maximising
337 amount of data within the subset. Within the subset there is very little variation in
338 temperature (<0.9°C) or pH (0.005 units), and a large range in salinity (3.50 PSU),
339 making it ideally suited to assess the Mg/Ca sensitivity to salinity (if pH is the
340 controlling carbonate system parameter). Using this subset of data and regressing
341 Mg/Ca against salinity only results in a salinity sensitivity of 3.3 ± 2.2 %/PSU ($p <$
342 0.01) (Fig. 3),

343

$$344 \text{Mg/Ca} = 1.75 \pm 1.81 \times \exp(0.033 \pm 0.022 \times S) \quad (1)$$

345

346 (RSE=0.30); incorporating both temperature and pH into the regression model results
347 in an identical salinity sensitivity of 3.3 ± 2.2 %/PSU ($p < 0.001$), indicating no effect
348 of covariance between predictor variables on the results. This result agrees well with
349 the culture study of Hönisch *et al.*, (2013), which suggested a salinity sensitivity of
350 3.3 ± 1.7 %/PSU for *G. ruber*, and is significantly lower than the coretop based

351 estimates of Ferguson *et al.* (2008), Arbueszowski *et al.* (2010), and Mathien-Blard
352 and Bassinot (2009).

353

354 Due to the strong covariance of salinity and $[\text{CO}_3^{2-}]$ within the Arabian
355 Sea/Bay of Bengal dataset ($r= 0.96$), it is not possible to constrain the effect of
356 salinity if $[\text{CO}_3^{2-}]$ is the controlling carbonate system parameter unless some
357 assumption of the sensitivity of Mg/Ca to $[\text{CO}_3^{2-}]$ is made (see section 3.6);
358 substituting $[\text{CO}_3^{2-}]$ for pH within the regression model results in insignificant terms
359 for both salinity and $[\text{CO}_3^{2-}]$.

360

361 *3.5 Sensitivity of Mg/Ca to temperature*

362 To constrain the sensitivity of Mg/Ca to temperature, we take a subset of the
363 global dataset with significantly lower variation in salinity (<0.6 PSU) and where the
364 covariance between temperature and salinity ($r = -0.09$), and temperature and pH ($r =$
365 -0.34) is considerably reduced. We opt for this salinity/pH range (36.1 to 37.0
366 PSU/8.06 to 8.12 pH units) as it gives the greatest number of data points ($n = 215$,
367 $\sim 50\%$ of the global dataset), while ensuring the maximum range in temperature (7.5
368 $^{\circ}\text{C}$) and the least covariance between predictor variables. The subset of data
369 comprises three previously published datasets (Anand *et al.*, 2003; Haarmann *et al.*,
370 2011; Babila *et al.*, 2014), and the newly generated data from the tropical Atlantic
371 (Fig. 6).

372

373 Regressing Mg/Ca against temperature results in a temperature sensitivity of
374 $6.0 \pm 0.8 \text{ \%}/^{\circ}\text{C}$ ($p < 10^{-15}$),

375

376
$$\text{Mg/Ca} = 1.08 \pm 0.25 \times \exp(0.060 \pm 0.008 \times T) \quad (2)$$

377

378 (RSE=0.45) (Fig. 6). Adding salinity and pH into the regression model results in an
379 identical temperature sensitivity of $6.0 \pm 0.7 \text{ \%/}^\circ\text{C}$ ($p < 10^{-15}$), indicating no influence
380 of covariance between temperature and salinity, and temperature and pH, on the
381 results. Substituting pH for $[\text{CO}_3^{2-}]$ results in a lower sensitivity of $5.4 \pm 0.9 \text{ \%/}^\circ\text{C}$ ($p <$
382 10^{-15}); however, temperature and $[\text{CO}_3^{2-}]$ covary within the subset of data ($r = 0.67$).
383 Consequently, this subset of data cannot be used to constrain the sensitivity of Mg/Ca
384 to temperature if $[\text{CO}_3^{2-}]$ is the controlling carbonate system parameter unless a
385 sensitivity to $[\text{CO}_3^{2-}]$ can be assumed (see section 3.6).

386

387 We performed an ‘extreme jackknife’ of the temperature regression to assess
388 whether the resulting temperature sensitivity is being significantly biased by any one
389 of the constituent datasets (SM). This test assesses whether the temperature sensitivity
390 given in Eq. 2 is biased by: (a) the Mg/Ca of a particular dataset being significantly
391 influenced by another factor that is not accounted for in the regression model, or (b) a
392 systematic offset between the habitat depth temperature in the time-period covered by
393 the trap samples at a particular site and the 0-50 m depth climatological temperature
394 at that site; the results demonstrate that no one particular dataset is significantly
395 biasing the results (Fig. 6b).

396

397 A key finding of our study is that the temperature sensitivity of $6.0 \pm 0.8 \text{ \%/}^\circ\text{C}$
398 given in Eq. 2 is significantly lower than the widely-applied $9.0 \pm 0.6 \text{ \%/}^\circ\text{C}$ sensitivity
399 of Dekens *et al.* (2002)/Anand *et al.* (2003); it is clear from Figure 6 that the
400 calibration of Dekens *et al.* (2002)/Anand *et al.* (2003) does not accurately describe

401 the dataset. Assuming a 0-25m habitat depth for this subset results in a lower
402 temperature sensitivity of 5.2 ± 0.8 %/°C (Eq. S5). The residual standard error of this
403 fit is, however, substantially higher than using a habitat depth of 0-50 m. The lower
404 temperature sensitivity in Eq. 2 compared to the 9.0 ± 0.6 %/°C sensitivity in the
405 calibration of Dekens *et al.* (2002)/Anand *et al.* (2003) is therefore not dependent on
406 the assumed habitat depth of *G. ruber* (w). Forcing the temperature sensitivity to a
407 higher value (i.e. 9%/°C) increases the residual standard error of fit (Fig. S7). Our
408 results do not support the relationship between Mg/Ca and temperature suggested by
409 Dekens *et al.* (2002)/Anand *et al.* (2003).

410

411 Regressing only the data from Anand *et al.*, (2003) against climatological
412 temperature results in a temperature sensitivity of 7.0 ± 1.2 %/°C (Eq. S6). Therefore,
413 the data of Anand *et al.*, (2003) do not support a temperature sensitivity of 9%/°C
414 when climatological temperature, rather than $\delta^{18}\text{O}_{\text{calcite-water}}$ temperature, is used. Note
415 that temperature and pH covary almost perfectly in the dataset of Anand *et al.*, (2003)
416 ($r = -0.98$), which may be the cause of the slightly higher apparent temperature
417 sensitivity in this dataset (see section 3.7 for further discussion on temperature-pH
418 covariance). Anand *et al.* (2003) pointed out that the $\delta^{18}\text{O}_{\text{calcite-water}}$ temperatures used
419 in their study were ~ 3 °C warmer than the measured CTD temperatures of the upper
420 1m of the water column during the winter months of the study period. The authors
421 suggested this may have been due to a sampling bias associated with warm-core
422 eddies. Our compilation demonstrates the data of Anand *et al.* (2003) are not
423 exceptional.

424

425 Now we will revisit the possible cause of this discrepancy by assessing the
426 application of different $\delta^{18}\text{O}_{\text{calcite-water}}$ calibrations, looking at the effects of $[\text{CO}_3^{2-}]$ on
427 $\delta^{18}\text{O}_{\text{calcite}}$ (Spero *et al.*, 1997), and exploring the potential for variability in the
428 salinity- $\delta^{18}\text{O}_{\text{water}}$ relationship (SM). As Figure S9 shows, the choice of $\delta^{18}\text{O}_{\text{calcite-water}}$
429 calibration makes little difference to the problem, with the seasonal range predicted in
430 $\delta^{18}\text{O}_{\text{calcite}}$ always $\sim 0.5\%$ greater than the range observed in foraminiferal $\delta^{18}\text{O}_{\text{calcite}}$.
431 Applying the $[\text{CO}_3^{2-}]$ - $\delta^{18}\text{O}$ relationship of Spero *et al.*, (1997), the seasonal variability
432 of $[\text{CO}_3^{2-}]$ in the Sargasso Sea can only explain 10% ($\sim 0.05\%$) of this discrepancy
433 (Fig. S10).

434

435 With choice of $\delta^{18}\text{O}_{\text{calcite-water}}$ calibration and carbonate chemistry changes
436 unable to adequately account for the discrepancy, we now assess the potential for a
437 systematic seasonal change in the salinity- $\delta^{18}\text{O}_{\text{water}}$ relationship; this could result in a
438 substantially larger change in $\delta^{18}\text{O}_{\text{water}}$ than suggested by the modest seasonal change
439 in salinity. LeGrande and Schmidt (2006) state that current salinity- $\delta^{18}\text{O}_{\text{water}}$
440 relationships are only applicable at a regional level, and these relationships may
441 change seasonally. Although no obvious seasonal cycle is apparent in the very limited
442 number of $\delta^{18}\text{O}_{\text{water}}$ measurements from the region, the data do display variability of
443 the magnitude required to explain the discrepancy ($\pm 0.7\%$) (Fig. S11). A systematic
444 seasonal change in $\delta^{18}\text{O}_{\text{water}}$ would therefore seem the most likely cause of the
445 discrepancy in $\delta^{18}\text{O}_{\text{calcite}}$, and explain why it is observed in multiple planktic
446 foraminiferal species simultaneously (Anand *et al.*, 2003).

447

448 *3.6 Sensitivity of Mg/Ca to the carbonate system*

449 The limited range in pH and $[\text{CO}_3^{2-}]$ within the dataset does not allow us to
450 use the same approach used to constrain the sensitivity to salinity and temperature.
451 Instead, to assess the sensitivity of Mg/Ca to pH we perform a multivariate regression
452 using the entire global dataset and prescribe the sensitivity of Mg/Ca to temperature
453 and salinity as $6.0 \pm 0.8 \text{ \%}/^\circ\text{C}$ and $3.3 \pm 2.2 \text{ \%}/\text{PSU}$ (see sections 3.5 and 3.6). We
454 account for the uncertainty in temperature and salinity sensitivity with Monte-Carlo
455 simulation. This approach results in a pH sensitivity of $-8.3 \pm 7.3 \text{ \%}/0.1 \text{ pH units}$ ($p <$
456 10^{-5}) (Fig. 7),

457

$$458 \text{ Mg/Ca} = \exp(0.060 \pm 0.008 \times T + 0.033 \pm 0.022 \times S - 0.83 \pm 0.73 \times (\text{pH} - 8) - 1.07 \pm 0.80) \quad (3)$$

459

460 (RSE=0.50). The large uncertainty associated with the pH sensitivity in Eq. 3 is
461 primarily due to the very small range in pH within the dataset (~ 0.13 units). This
462 result is in very good agreement with an exponential fit to the *G. ruber* (w) culture
463 experiments of Kisakürek *et al.*, (2008) and Evans *et al.*, (2016), which yields a pH
464 sensitivity of $-9.3 \pm 4.1 \text{ \%}/0.1 \text{ pH units}$ (Eq. S11) (Fig. 7). Our estimate of the
465 sensitivity of Mg/Ca to pH is entirely consistent with the results of the culture data of
466 Kisakürek *et al.*, (2008)/Evans *et al.*, (2016).

467

468 If we consider that $[\text{CO}_3^{2-}]$ is the controlling carbonate system parameter we
469 must take a different approach than that used to estimate the sensitivity to pH. This is
470 because the salinity sensitivity used to account for the effects of salinity in the
471 regression model is derived from the Arabian Sea/Bengal dataset, in which salinity
472 and $[\text{CO}_3^{2-}]$ covary strongly. Furthermore, there is also covariance between $[\text{CO}_3^{2-}]$
473 and temperature in the subset of data used to derive the sensitivity to temperature in

474 Eq. 2. Instead we must assume a sensitivity to $[\text{CO}_3^{2-}]$ and use this assumed
475 sensitivity to $[\text{CO}_3^{2-}]$ to calculate a sensitivity to salinity; we can then use the assumed
476 sensitivity to $[\text{CO}_3^{2-}]$ and calculated sensitivity to salinity to derive the sensitivity of
477 Mg/Ca to temperature if $[\text{CO}_3^{2-}]$ is the controlling parameter.

478

479 Regressing the data from the culture experiments of Kisakürek *et al.*,
480 (2008)/Evans *et al.*, (2016) against $[\text{CO}_3^{2-}]$ results in a sensitivity of -0.24 ± 0.12
481 $\%/\mu\text{mol kg}^{-1}$ (Eq. S12; Fig. S12), within error of the $-0.35 \pm 0.12 \%/\mu\text{mol kg}^{-1}$
482 suggested by multivariate regression of the global dataset (Eq. S4). Taking a subset of
483 data from the Arabian Sea/Bay of Bengal dataset from the same temperature range
484 used to calculate the sensitivity to salinity in Eq. 1 (28 – 29 °C), and regressing the
485 data against salinity with a prescribed sensitivity to $[\text{CO}_3^{2-}]$ of $-0.24 \pm 0.12 \%/\mu\text{mol kg}^{-1}$
486 results in a salinity sensitivity of $5.0 \pm 3.0 \%/PSU$ ($p < 0.001$). Incorporating
487 temperature within the regression model results in a very similar salinity sensitivity of
488 $5.1 \pm 2.8 \%/PSU$ ($p < 10^{-5}$). Prescribing the salinity sensitivity of $5.0 \pm 3.0 \%/PSU$, and
489 the $[\text{CO}_3^{2-}]$ sensitivity of $-0.24 \pm 0.12 \%/\mu\text{mol kg}^{-1}$ in a multivariate regression of the
490 entire dataset results in a temperature sensitivity of $6.7 \pm 0.8 \%/^{\circ}\text{C}$ ($p < 10^{-15}$),

491

$$492 \text{Mg/Ca} = \exp(0.067 \pm 0.008 \times T + 0.050 \pm 0.030 \times S - 0.0024 \pm 0.0012 \times [\text{CO}_3^{2-}] - 1.37 \pm 1.31)$$

493 (4)

494

495 (RSE=0.50), similar to the temperature sensitivity if pH is the controlling parameter
496 (Eq. 3). Regressing the subset of data with very little variation in salinity (< 0.6 PSU)
497 used to calculate the temperature sensitivity in section 3.5 against temperature with a
498 prescribed sensitivity to $[\text{CO}_3^{2-}]$ of $-0.24 \pm 0.12 \%/\mu\text{mol kg}^{-1}$ results in an identical

499 (within error) temperature sensitivity of $7.0 \pm 0.9 \text{ \%}/^\circ\text{C}$. This confirms the temperature
500 sensitivity given in Eq. 4, without necessitating an assumption of the sensitivity to
501 salinity. Application of a lower $[\text{CO}_3^{2-}]$ sensitivity, as suggested for *G. ruber* (pink)
502 (Allen *et al.*, 2016), has very little effect on the resulting temperature and salinity
503 sensitivities (SM).

504

505 3.7 Reconciling sediment trap and culture temperature sensitivity estimates

506 The temperature sensitivities indicated by the sediment trap data, i.e. 6.0 ± 0.8
507 $\text{\%/}^\circ\text{C}$ if pH is the controlling parameter, and $6.7 \pm 0.8 \text{\%/}^\circ\text{C}$ if $[\text{CO}_3^{2-}]$ is the controlling
508 parameter, are lower than the temperature sensitivity of $8 \pm 3 \text{\%/}^\circ\text{C}$ inferred from the
509 culturing experiment of Kisakürek *et al.*, (2008) (Fig. 8). One way by which the
510 sediment trap and culture data can be reconciled is if the influence of temperature on
511 the dissociation constant of water ($K_w = [\text{H}^+][\text{OH}^-]$) is considered. As K_w changes as a
512 function of temperature, the pH of water decreases with increasing temperature by ~
513 0.015 pH units/ $^\circ\text{C}$, without changing the ratio of Alk/DIC (Millero, 1995). Hence, in
514 the culture experiments of Kisakürek *et al.*, (2008) temperature and pH covary
515 perfectly ($r > 0.99$), with a 0.18 pH unit decrease from coldest to warmest sample. If
516 the culture data of Kisakürek *et al.*, (2008) are normalised to a pH of 8.05 (the mean
517 value within the sediment trap dataset) to remove the internal shift of pH due to
518 temperature, using a pH sensitivity of $-8.3 \text{\%/}0.1 \text{ pH units}$ derived from the sediment
519 trap dataset (Eq. 3), the Kisakürek *et al.*, (2008) data suggest a lower temperature
520 sensitivity of $6.3 \pm 1.9 \text{\%/}^\circ\text{C}$ ($p < 0.01$) (Fig. 8),

521

$$522 \text{Mg/Ca} = 0.97 \pm 0.50 \times \exp(0.063 \pm 0.019 \times T) \quad (5)$$

523

524 (RSE=0.36; n=5), in excellent agreement with the temperature sensitivity indicated by
525 the sediment trap dataset if pH is the controlling carbonate system parameter (Eq. 3;
526 Fig. 8). Using the pH sensitivity of -9.3 ± 4.6 %/0.1 pH units suggested by the pH
527 experiments to normalise the culture data instead, results in an identical (within error)
528 temperature sensitivity of 6.2 ± 1.9 %/°C ($p < 0.01$). Accounting for the influence of
529 temperature on the dissociation constant of water (K_w) within the culturing
530 experiments thus allows the culture and sediment trap datasets to be reconciled if pH
531 is the controlling carbonate system parameter. If $[\text{CO}_3^{2-}]$ is the controlling carbonate
532 system parameter, the sediment trap and culture data cannot be reconciled as the ratio
533 of Alk/DIC (and thus $[\text{CO}_3^{2-}]$) is not changing in the temperature experiment of
534 Kisakürek *et al.*, (2008). Based on our current understanding of foraminiferal
535 calcification mechanisms (e.g. Erez *et al.*, 2003; de Nooijer *et al.*, 2009), Evans *et al.*,
536 (2016) argued that pH is the carbonate system parameter that influences foraminiferal
537 Mg/Ca (SM), and recent work has revealed foraminifera actively pump protons
538 during calcification (Toyofuku *et al.*, 2017). Our results provisionally support this
539 inference, as this would allow the sediment trap and culture data to be reconciled.

540

541 3.8 Proposed calibrations

542 We propose the following calibration for the conversion of *G. ruber* (w)
543 Mg/Ca to temperature if pH is the controlling carbonate system parameter,

544

$$545 \text{Mg/Ca} = \exp(0.060 \pm 0.008 \times T + 0.033 \pm 0.022 \times S - 0.83 \pm 0.73 \times (\text{pH} - 8) - 1.07 \pm 0.80) \quad (3)$$

546

547 (RSE=0.50), and the following calibration if $[\text{CO}_3^{2-}]$ is the controlling carbonate
548 system parameter,

549

$$550 \quad \text{Mg/Ca} = \exp(0.067 \pm 0.008 \times T + 0.050 \pm 0.030 \times S - 0.0024 \pm 0.0012 \times [\text{CO}_3^{2-}] - 1.37 \pm 1.31)$$

551 (4)

552

553 (RSE=0.50). As discussed above, we suggest that pH is most likely to be the
554 controlling carbonate system parameter as this allows the reconciliation of the culture
555 experiment and sediment trap datasets, but further culturing work is needed to test this
556 assertion.

557

558 *3.9 Sources of noise within the calibration*

559 Significant noise can be seen in the sediment trap Mg/Ca dataset (Fig. 8),
560 with ~30% of the variance unaccounted for by T, S and the carbonate system. Here
561 we assess how much of this noise relates to (i) the use of climatological temperature
562 and (ii) different size fractions within the dataset.

563

564 To assess how much noise may be explained by the use of climatological
565 temperatures we simulate synthetic foraminiferal samples using both CTD
566 temperature and WOA13 temperature for the same period of time, and examine the
567 difference expected in Mg/Ca between these samples (SM). We utilise data from the
568 Sargasso Sea, which is the only trap site with continuous CTD data for the time
569 interval covered by the sediment samples, and simulate samples broadly
570 representative of the actual samples analysed by Anand *et al.* (2003) and Babila *et al.*
571 (2014). We then calculate the residual Mg/Ca based on the difference in temperature
572 between the WOA-synthetic foraminiferal samples and the CTD-synthetic
573 foraminiferal samples and compare this to the residual of the measured Mg/Ca data

574 from the Sargasso Sea sediment trap site. The results show that the residual in
575 measured Mg/Ca data is significantly higher than expected based on the uncertainty
576 introduced by using climatological temperature alone ($p < 10^{-7}$) (Fig. S15); however,
577 ~40% of noise can be explained by the use of climatological temperature. If the
578 Sargasso Sea dataset is representative of the wider trap/tow dataset, substantial
579 improvements in the precision of the calibration could be made if in-situ temperatures
580 were collected along with foraminiferal samples.

581

582 Another source of noise may relate to ‘biological’ variability. One aspect of
583 biological variability that might be constrained is the influence of size fractions within
584 the global dataset. The mean size of foraminiferal sample within the dataset is 300
585 μm , and 95% of samples fall into the 200 to 400 μm range of mean test size. To test if
586 it is possible to systematically correct for variations in test size, we use the
587 relationship between test size and Mg/Ca given in Figure 4e ($0.35 \text{ mmol mol}^{-1}/100$
588 μm) to normalise all sediment trap and plankton tow data within the dataset to the
589 same size (300 μm). Regressing the size normalised Mg/Ca against temperature,
590 salinity and $\text{pH}/[\text{CO}_3^{2-}]$ increases the residual standard error of fit compared to
591 regressions of the uncorrected data. Incorporating test size as a predictor variable
592 within the regression model returns an insignificant coefficient for test size. Thus,
593 while test size variability might be causing much of the noise, such effects cannot
594 easily be corrected.

595

596 **4. Implications for tropical SST during the LGM**

597

598 We apply our new multivariate calibration models to previously published *G.*
599 *ruber* (w) Mg/Ca data from multiple core sites located in the tropical Pacific, Indian
600 and Atlantic Oceans covering the Last Glacial Maximum (LGM) (SM). Applying the
601 calibration given in Eq. 3, which assumes pH is the controlling carbonate system
602 parameter, results in a tropical ocean cooling of 3.5 ± 1.6 °C (2σ , accounting for
603 Mg/Ca variability only) if no change in salinity or pH is accounted for (Fig. 9). If the
604 1.15 PSU whole ocean increase in salinity during the LGM (Adkins *et al.*, 2002) is
605 included, the magnitude of cooling increases to 4.2 ± 1.6 °C. However, if a 0.13 unit
606 surface ocean pH increase (SM) is also accounted for, the magnitude of cooling is
607 reduced to 2.4 ± 1.6 °C. This calculation demonstrates that the combined pH and
608 salinity influence in Eq. 3 reduces the inferred temperature change by about a third.
609 We note that while this value is similar to the value (2.3 ± 1.3 °C) obtained using the
610 calibration of Dekens *et al.* (2002)/Anand *et al.* (2003) (Fig. 9), this similarity is not a
611 confirmation of the calibration of Dekens *et al.* (2002)/Anand *et al.* (2003), which has
612 a higher temperature sensitivity and does not account for changes in salinity or
613 carbonate chemistry.

614

615 Applying the calibration given in Eq. 4, which assumes $[\text{CO}_3^{2-}]$ is the
616 controlling carbonate system parameter, results in a cooling of 3.1 ± 1.4 °C (2σ) if no
617 change in salinity or $[\text{CO}_3^{2-}]$ is considered (Fig. 9). If the 1.15 PSU whole ocean
618 increase in salinity is accounted for, the magnitude of cooling during the LGM
619 increases to 4.0 ± 1.4 °C. However, if a 69 $\mu\text{mol/kg}$ surface ocean $[\text{CO}_3^{2-}]$ increase is
620 also included (SM), the magnitude of cooling is reduced to 1.5 ± 1.4 °C. The
621 substantial effect of including the carbonate ion change on the temperature estimate

622 reflects the strong influence of carbonate ion in Eq. 4, where it accounts for a
623 significantly greater weighting than temperature for LGM conditions.

624

625 These scenarios are not intended as a thorough estimation of LGM
626 temperature change, but instead serve only to highlight that salinity and carbonate
627 chemistry have a substantial effect on reconstructed temperature, and the necessity of
628 obtaining regional salinity and pH/[CO₃²⁻] estimates for robust SST reconstruction
629 using Mg/Ca. In addition to the secondary influences on Mg uptake into foraminiferal
630 calcite, the effects of dissolution (usually expressed as a function of bottom-water
631 carbonate ion saturation, ΔCO₃²⁻) on Mg/Ca must also be accounted for in
632 temperature reconstructions from fossil foraminifera (Regenberg *et al.*, 2014).
633 Uncertainty in reconstructed temperature change from Mg/Ca will therefore be
634 dependent on the uncertainty of the sensitivities of Mg/Ca to temperature, salinity and
635 the carbonate system within the calibration, the uncertainty in past changes in salinity
636 and pH/[CO₃²⁻], as well as both the uncertainty in relationship between Mg/Ca and
637 dissolution, and the uncertainty in past changes in bottom- (or pore-) water carbonate
638 chemistry.

639

640 **5. Conclusions**

641

642 This study utilises 440 sediment trap/plankton tow samples from 20 sites in
643 Atlantic, Pacific and Indian basins to provide the most comprehensive field based
644 calibration for Mg/Ca in *G. ruber* (white) to date. The temperature sensitivity within
645 our calibration of 6.0% per °C (assuming pH is the controlling carbonate system
646 parameter) or 6.7% per °C (assuming [CO₃²⁻] is the controlling carbonate system

647 parameter) is significantly lower than the widely-applied temperature sensitivity of
648 9% per °C. The significant effects of salinity (with a sensitivity of 3.3% or 5% per
649 PSU, depending on the controlling carbonate system parameter) and carbonate
650 chemistry (with a sensitivity of -8.3% per 0.1 pH units or -0.24% per $\mu\text{mol/kg}$ $[\text{CO}_3^{2-}]$
651]) on Mg/Ca in *G. ruber* (white) complicate the use of Mg/Ca as a paleothermometer.

652

653 Applying our calibration model which assumes pH is the controlling carbonate
654 system parameter (we provisionally suggest pH is most likely to be the controlling
655 parameter), without considering changes in salinity and carbonate chemistry, results
656 in a cooling of $\sim 3.5^\circ\text{C}$ during the LGM; if whole ocean changes in salinity and
657 carbonate chemistry are accounted for the cooling is reduced to $\sim 2.3^\circ\text{C}$. Applying our
658 calibration model which assumes $[\text{CO}_3^{2-}]$ is the controlling carbonate system
659 parameter, without considering changes in salinity and carbonate chemistry, results in
660 a cooling of $\sim 3.1^\circ\text{C}$ during the LGM; if whole ocean changes in salinity and
661 carbonate chemistry are accounted for the cooling is reduced to $\sim 1.5^\circ\text{C}$. The
662 substantial influence of salinity and carbonate chemistry on Mg/Ca necessitates
663 independent estimates of salinity and carbonate chemistry for reliable temperature
664 reconstruction. While boron isotopes may offer a viable tool to account for changes in
665 carbonate chemistry, the lack of a quantitative salinity proxy currently adds a currently-
666 unquantifiable uncertainty into Mg/Ca-based temperature estimates.

667

668 Future efforts to further improve the Mg/Ca paleothermometer should include
669 (i) culture experiments to assess whether it is pH or $[\text{CO}_3^{2-}]$ that controls Mg/Ca, and
670 determine the exact form and sensitivity of this relationship (ii) studies to ascertain if
671 the secondary influences on Mg/Ca in *G. ruber* (white) are as pronounced in other

672 planktic foraminiferal species and, (iii) the development and refinement of an
673 independent salinity proxy.

674

675 *Acknowledgments*

676 This research was funded by NSF grant NSF-OCE 1260696 awarded to S.
677 Weldeab and D.W. Lea. We thank Ralf Schiebel for discussions regarding
678 foraminiferal ecology, Birgit Gaye for providing sediment trap samples from the Bay
679 of Bengal, Bobbi Conard for sampling archived sediment trap samples from the
680 Arabian Sea, Minda Monteagudo for help in the preparation of foraminiferal samples
681 for trace element analysis, Ryan Bu for assistance with ICP-MS analysis, Siv Lauvset
682 for discussions regarding carbonate chemistry data, and Damian Loher for assistance
683 producing the temporally resolved carbonate chemistry estimates. Conversations with
684 David Evans and Rosanna Greenop helped guide our thinking regarding potential
685 solutions to the problems raised by the influence of carbonate chemistry on Mg/Ca.
686 Insightful comments from the Editor (Heather Stoll), Michael Henehan, and an
687 anonymous reviewer very much improved previous versions of this manuscript.

688

689 *References*

- 690 Adkins, J.F., McIntyre, K., Schrag, D.P., 2002. The salinity, temperature, and $\delta^{18}\text{O}$ of the glacial deep
691 ocean. *Science* 289, 1769–1773. doi:10.1126/science.1076252
- 692 Allen, K.A., Hönisch, B., Eggins, S.M., Haynes, L.L., Rosenthal, Y., Yu, J., 2016. Trace element
693 proxies for surface ocean conditions: A synthesis of culture calibrations with planktic
694 foraminifera. *Geochimica et Cosmochimica Acta* 193, 197–221. doi:10.1016/j.gca.2016.08.015
- 695 Anand, P., Elderfield, H., Conte, M.H., 2003. Calibration of Mg/Ca thermometry in planktonic
696 foraminifera from a sediment trap time series. *Paleoceanography* 18, 1050.
697 doi:10.1029/2002PA000846
- 698 Arbuszewski, J., deMenocal, P., Kaplan, A., Farmer, E.C., 2010. On the fidelity of shell-derived
699 $\delta^{18}\text{O}$ seawater estimates. *Earth and Planetary Science Letters* 300, 185–196.
700 doi:10.1016/j.epsl.2010.10.035
- 701 Babila, T.L., Rosenthal, Y., Conte, M.H., 2014. Evaluation of the biogeochemical controls on B/Ca of
702 Globigerinoides ruber white from the Oceanic Flux Program, Bermuda. *Earth and Planetary
703 Science Letters* 404, 67–76. doi:10.1016/j.epsl.2014.05.053
- 704 Boussetta, S., Bassinot, F., Sabbatini, A., Caillon, N., Nouet, J., Kallel, N., Rebaubier, H.,
705 Klinkhammer, G., Labeyrie, L., 2011. Diagenetic Mg-rich calcite in Mediterranean sediments:
706 Quantification and impact on foraminiferal Mg/Ca thermometry. *Marine Geology* 280, 195–204.

707 doi:10.1016/j.margeo.2010.12.011
708 Boyer, T.P., J.I. Antonov, O.K. Baranova, C. Coleman, H.E. Garcia, A. Grodsky, D.R. Johnson, R.A.
709 Locarnini, A.V. Mishonov, T.D. O'Brien, C.R. Paver, J.R. Reagan, D. Seidov, I.V. Smolyar, M.M.
710 Zweng, 2013, World Ocean Database 2013. Sydney Levitus, Ed.; Alexey Mishonov, Technical
711 Ed.; NOAA Atlas NESDIS 72, 209 pp.
712 de Nooijer, L.J., Toyofuku, T., Kitazato, H., 2009. Foraminifera promote calcification by elevating
713 their intracellular pH. *Proceedings of the National Academy of Sciences* 106, 15374–15378.
714 doi:10.1073/pnas.0904306106
715 Dekens, P.S., Lea, D.W., Pak, D.K., Spero, H.J., 2002. Core top calibration of Mg/Ca in tropical
716 foraminifera: Refining paleotemperature estimation. *Geochem. Geophys. Geosyst.* 3, 1–29.
717 doi:10.1029/2001GC000200
718 Efron, B., 1979. Computers and the theory of statistics: thinking the unthinkable. *SIAM review* 21,
719 460–480. doi:10.1137/1021092
720 Erez, J., 2003. The Source of Ions for Biomineralization in Foraminifera and Their Implications for
721 Paleoceanographic Proxies. *Reviews in Mineralogy and Geochemistry* 54, 115–149.
722 doi:10.2113/0540115
723 Evans, D., Wade, B.S., Henehan, M., Erez, J., Müller, W., 2016. Revisiting carbonate chemistry
724 controls on planktic foraminifera Mg/Ca: implications for sea surface temperature and hydrology
725 shifts over the Paleocene–Eocene Thermal Maximum and Eocene–Oligocene Transition. *Clim.*
726 *Past* 12, 819–835. doi:10.5194/cp-12-819-2016
727 Fallet, U., Brummer, G.-J., Zinke, J., Vogels, S., Ridderinkhof, H., 2010. Contrasting seasonal fluxes
728 of planktonic foraminifera and impacts on paleothermometry in the Mozambique Channel
729 upstream of the Agulhas Current. *Paleoceanography* 25, PA4223. doi:10.1029/2010PA001942
730 Ferguson, J.E., Henderson, G.M., Kucera, M., Rickaby, R.E.M., 2008. Systematic change of
731 foraminiferal Mg/Ca ratios across a strong salinity gradient. *Earth and Planetary Science Letters*
732 265, 153–166. doi:10.1016/j.epsl.2007.10.011
733 Fischer, G., Romero, O., Merkel, U., Donner, B., Iversen, M., Nowald, N., Ratmeyer, V., Ruhland, G.,
734 Klann, M., Wefer, G., 2016. Deep ocean particle flux in the coastal upwelling off Mauritania from
735 1988 to 2012: variability on seasonal to decadal timescales. *Biogeosciences*, 13, 3071–3090.
736 Friedrich, O., Schiebel, R., Wilson, P.A., Weldeab, S., Beer, C.J., Cooper, M.J., Fiebig, J., 2012.
737 Influence of test size, water depth, and ecology on Mg/Ca, Sr/Ca, $\delta^{18}\text{O}$ and $\delta^{13}\text{C}$ in nine modern
738 species of planktic foraminifers. *Earth and Planetary Science Letters* 319–320, 133–145.
739 doi:10.1016/j.epsl.2011.12.002
740 Haarmann, T., Hathorne, E.C., Mohtadi, M., Groeneveld, J., Kölling, M., Bickert, T., 2011. Mg/Ca
741 ratios of single planktonic foraminifer shells and the potential to reconstruct the thermal
742 seasonality of the water column. *Paleoceanography* 26, PA3218. doi:10.1029/2010PA002091
743 Hemleben, Ch., Spindler, M., Anderson, O.R., 1989. *Modern Planktonic Foraminifera*. pp.363.
744 Springer (New York, Berlin)
745 Henehan, M. J., Rae, J. W. B., Foster, G. L., Erez, J., Prentice, K. C., Kucera, M., Bostok, H. C.,
746 Martínez-Botí, M. A., Milton, A. J., Wilson, P. A., Marshall, B. J., Elliot, T., 2013. Calibration of
747 the boron isotope proxy in the planktonic foraminifera *Globigerinoides ruber* for use in palaeo-
748 CO₂ reconstruction. *Earth and Planetary Science Letters* 364, 111–122.
749 Henehan, M.J., Evans, D., Shankle, M., Burke, J.E., Foster, G.L., Aganostou, E., Chalk, T.B., Stewart,
750 J.A., Alt, C.H.S., Durrant, J., Hull, P.M., 2017. Size-dependent response of foraminiferal
751 calcification to seawater carbonate chemistry. *Biogeosciences*, 14, 3287–3308.
752 Hertzberg, J.E., Schmidt, M.W., 2013. Refining *Globigerinoides ruber* Mg/Ca paleothermometry in the
753 Atlantic Ocean. *Earth and Planetary Science Letters* 383, 123–133.
754 doi:10.1016/j.epsl.2013.09.044
755 Honjo, S., Dymond, J., Prell, W., Ittekkot, V., 1999. Monsoon-controlled export fluxes to the interior
756 of the Arabian Sea. *Deep Sea Research Part II* 46, 1859–1902. doi:10.1016/S0967-
757 0645(99)00047-8
758 Hönisch, B., Allen, K.A., Lea, D.W., Spero, H.J., Eggins, S.M., Arbuszewski, J., deMenocal, P.,
759 Rosenthal, Y., Russell, A.D., Elderfield, H., 2013. The influence of salinity on Mg/Ca in planktic
760 foraminifers – Evidence from cultures, core-top sediments and complementary $\delta^{18}\text{O}$. *Geochimica*
761 *et Cosmochimica Acta* 121, 196–213. doi:10.1016/j.gca.2013.07.028
762 Huang, K.-F., You, C.-F., Lin, H.-L., Shieh, Y.-T., 2008. In situ calibration of Mg/Ca ratio in
763 planktonic foraminiferal shell using time series sediment trap: A case study of intense dissolution
764 artifact in the South China Sea. *Geochem. Geophys. Geosyst.* 9, Q04016.
765 doi:10.1029/2007GC001660
766 Key, R.M., Olsen, A., van Heuven, S., Lauvset, S.K., 2015. Global Ocean Data Analysis Project,

767 Version 2 (GLODAPv2). ORNL/CDIAC-162. doi:10.3334/CDIAC/OTG
768 Khider, D., Huerta, G., Jackson, C., Stott, L.D., Emile-Geay, J., 2015. A Bayesian, multivariate
769 calibration for Globigerinoides ruber Mg/Ca. *Geochem. Geophys. Geosyst.* 16, 2916–2932.
770 doi:10.1002/2015GC005844
771 Kisakürek, B., Eisenhauer, A., Böhm, F., Garbe-Schönberg, D., Erez, J., 2008. Controls on shell
772 Mg/Ca and Sr/Ca in cultured planktonic foraminiferan, Globigerinoides ruber (white). *Earth and
773 Planetary Science Letters* 273, 260–269. doi:10.1016/j.epsl.2008.06.026
774 Landschützer, P., Gruber, N., Bakker, D. C. E., Schuster, U., 2014a. Recent variability of the global
775 ocean carbon sink, *Global Biogeochem. Cycles*, 28, 927–949, doi:10.1002/2014GB004853.
776 Landschützer, P., Gruber, N., Bakker, D. C. E., Schuster, U., 2014b. An observation-based global
777 monthly gridded sea surface pCO₂ product from 1998 through 2011 and its monthly climatology.
778 http://cdiac.ornl.gov/ftp/oceans/spco2_1998_2011_ETH_SOM-FFN. Carbon Dioxide Information
779 Analysis Center, Oak Ridge National Laboratory, US Department of Energy, Oak Ridge,
780 Tennessee. doi: 10.3334/CDIAC/OTG.SPCO2_1998_2011_ETH_SOM-FFN
781 Lauvset, S.K., Key, R.M., Olsen, A., 2016. A new global interior ocean mapped climatology: the 1°×
782 1° GLODAP version 2. *Earth Syst. Sci. Data*. doi:10.3334/CDIAC/OTG.NDP093_GLODAPv2
783 Lea, D.W., 2000. Climate Impact of Late Quaternary Equatorial Pacific Sea Surface Temperature
784 Variations. *Science* 289, 1719–1724. doi:10.1126/science.289.5485.1719
785 Lea, D.W., Mashiotta, T.A., Spero, H.J., 1999. Controls on magnesium and strontium uptake in
786 planktonic foraminifera determined by live culturing. *Geochimica et Cosmochimica Acta* 63,
787 2369–2379. doi:10.1016/S0016-7037(99)00197-0
788 Lee, K., Tong, L.T., Millero, F.J., Sabine, C.L., Dickson, A.G., Goyet, C., Park, G.-H., Wanninkhof,
789 R., Feely, R.A., Key, R.M., 2006. Global relationships of total alkalinity with salinity and
790 temperature in surface waters of the world's oceans. *Geophys. Res. Lett.* 33, L19605.
791 doi:10.1029/2006GL027207
792 LeGrande, A. N. and Schmidt, G. A. (2006). Global gridded data set of the oxygen isotopic
793 composition in seawater. *Geophys. Res. Lett.* 33(12):L12604.
794 Mathien-Blard, E., Bassinot, F., 2009. Salinity bias on the foraminifera Mg/Ca thermometry:
795 Correction procedure and implications for past ocean hydrographic reconstructions. *Geochem.
796 Geophys. Geosyst.* 10, Q12011. doi:10.1029/2008GC002353.
797 McConnell, M.C., Thunell, R.C., 2005. Calibration of the planktonic foraminiferal Mg/Ca
798 paleothermometer: Sediment trap results from the Guaymas Basin, Gulf of California.
799 *Paleoceanography* 20, PA2016. doi:10.1029/2004PA001077
800 Mohtadi, M., Prange, M., Oppo, D.W., De Pol-Holz, R., Merkel, U., Zhang, X., Steinke, S., Lückge,
801 A., 2014. North Atlantic forcing of tropical Indian Ocean climate. *Nature* 509, 76–80.
802 doi:10.1038/nature13196
803 Mohtadi, M., Steinke, S., Groeneveld, J., Fink, H.G., Rixen, T., Hebbeln, D., Donner, B., Herunadi, B.,
804 2009. Low-latitude control on seasonal and interannual changes in planktonic foraminiferal flux
805 and shell geochemistry off south Java: A sediment trap study. *Paleoceanography* 24, PA1201.
806 doi:10.1029/2008PA001636
807 Nürnberg, D., Bijma, J., Hemleben, C., 1996. Assessing the reliability of magnesium in foraminiferal
808 calcite as a proxy for water mass temperatures. *Geochimica et Cosmochimica Acta* 60, 803–814.
809 doi:10.1016/0016-7037(95)00446-7
810 Pak, D.K., Lea, D.W., Kennett, J.P., 2004. Seasonal and interannual variation in Santa Barbara Basin
811 water temperatures observed in sediment trap foraminiferal Mg/Ca. *Geochem. Geophys. Geosyst.*
812 5, Q12008. doi:10.1029/2004GC000760
813 Regenberg, M., Regenberg, A., Garbe-Schönberg, D., Lea, D.W., 2014. Global dissolution effects on
814 planktonic foraminiferal Mg/Ca ratios controlled by the calcite-saturation state of bottom waters.
815 *Paleoceanography* 29, 127–142. doi:10.1002/2013PA002492
816 Rosenthal, Y., Boyle, E.A., Slowey, N., 1997. Temperature control on the incorporation of magnesium,
817 strontium, fluorine, and cadmium into benthic foraminiferal shells from Little Bahama Bank:
818 Prospects for thermocline paleoceanography. *Geochimica et Cosmochimica Acta* 61, 3633–3643.
819 doi:10.1016/S0016-7037(97)00181-6
820 Russell, A.D., Hönisch, B., Spero, H.J., Lea, D.W., 2004. Effects of seawater carbonate ion
821 concentration and temperature on shell U, Mg, and Sr in cultured planktonic foraminifera.
822 *Geochimica et Cosmochimica Acta* 68, 4347–4361. doi:10.1016/j.gca.2004.03.013
823 Schmidt, M.W., Lynch-Stieglitz, J., 2011. Florida Straits deglacial temperature and salinity change:
824 Implications for tropical hydrologic cycle variability during the Younger Dryas.
825 *Paleoceanography* 26, 1–16. doi:10.1029/2011PA002157
826 Spero, H. J., Bijma, J., Lea, D.W., Bemis, B.E., 1997. Effect of seawater carbonate concentration on

827 foraminiferal carbon and oxygen isotopes. *Nature* 390, 497-500.
828 Toyofuku, T., Matsuo, M. Y., de Nooijer, L. J., Nagai, Y., Kawada, S., Fujita, K., Reichart, G-J.,
829 Nomaki, H., Tsuchiya, M., Sakaguchi, H., Kitazato, H., 2017. Proton pumping accompanies
830 calcification in foraminifera. *Nature Communications* 8, 14145. DOI: 10.1038.
831 Unger, D., Ittekkot, V., Schäfer, P., Tiemann, J., Reschke, S., 2003. Seasonality and interannual
832 variability of particle fluxes to the deep Bay of Bengal: influence of riverine input and
833 oceanographic processes. *Deep Sea Research Part II: Topical Studies in Oceanography* 50, 897–
834 923. doi:10.1016/S0967-0645(02)00612-4
835 Wang, L., 2000. Isotopic signals in two morphotypes of *Globigerinoides ruber* (white) from the South
836 China Sea: implications for monsoon climate change during the last glacial cycle.
837 *Palaeogeography* 161, 381–394. doi:10.1016/S0031-0182(00)00094-8
838 Weldeab, S., Lea, D.W., Schneider, R.R., Andersen, N., 2007. 155,000 Years of West African
839 Monsoon and Ocean Thermal Evolution. *Science* 316, 1303–1307. doi:10.1126/science.1140461
840

841

842

843

844

845

846

847

848

849

850

851

852

853

854

855

856

857

858

859

860

861

862

Table 1 Published temperature sensitivities¹ for *G. ruber* (white)²

Reference	Method	Temperature sensitivity (%) [*]
Lea <i>et al.</i> , 2000	Coretops, equatorial Pacific	8.9±1.4
Dekens <i>et al.</i> , 2002	Coretops, multivariate fit accounting for core depth	9±1.5
Anand <i>et al.</i> , 2003	Multi-species, sediment trap, Sargasso Sea, $\delta^{18}\text{O}$ temperature	9.0±0.6
Anand <i>et al.</i> , 2003	250-350 μm , sediment trap, Sargasso Sea, $\delta^{18}\text{O}$ temperature	10±2
Anand <i>et al.</i> , 2003	350-500 μm , sediment trap, Sargasso Sea, $\delta^{18}\text{O}$ temperature	8.5±1.2
McConnell & Thunell, 2005	Sediment trap, Gulf of California, satellite temperature	6.8
Kisakürek <i>et al.</i> , 2008	Laboratory cultures	8±3
Mohtadi <i>et al.</i> , 2009	Sediment trap, Java, satellite temperature	8.4
Mohtadi <i>et al.</i> , 2009	Sediment trap, Java, $\delta^{18}\text{O}$ temperature	6.6
Khider <i>et al.</i> , 2015	Coretops, Bayesian multivariate fit accounting for salinity, and bottom water carbonate ion saturation	8.7±0.9

¹Excluding studies where the temperature sensitivity was assumed

²Including one study combining multiple species of planktonic foraminifera

* 95% confidence interval

863

864

865

866

867

868

869

870

871

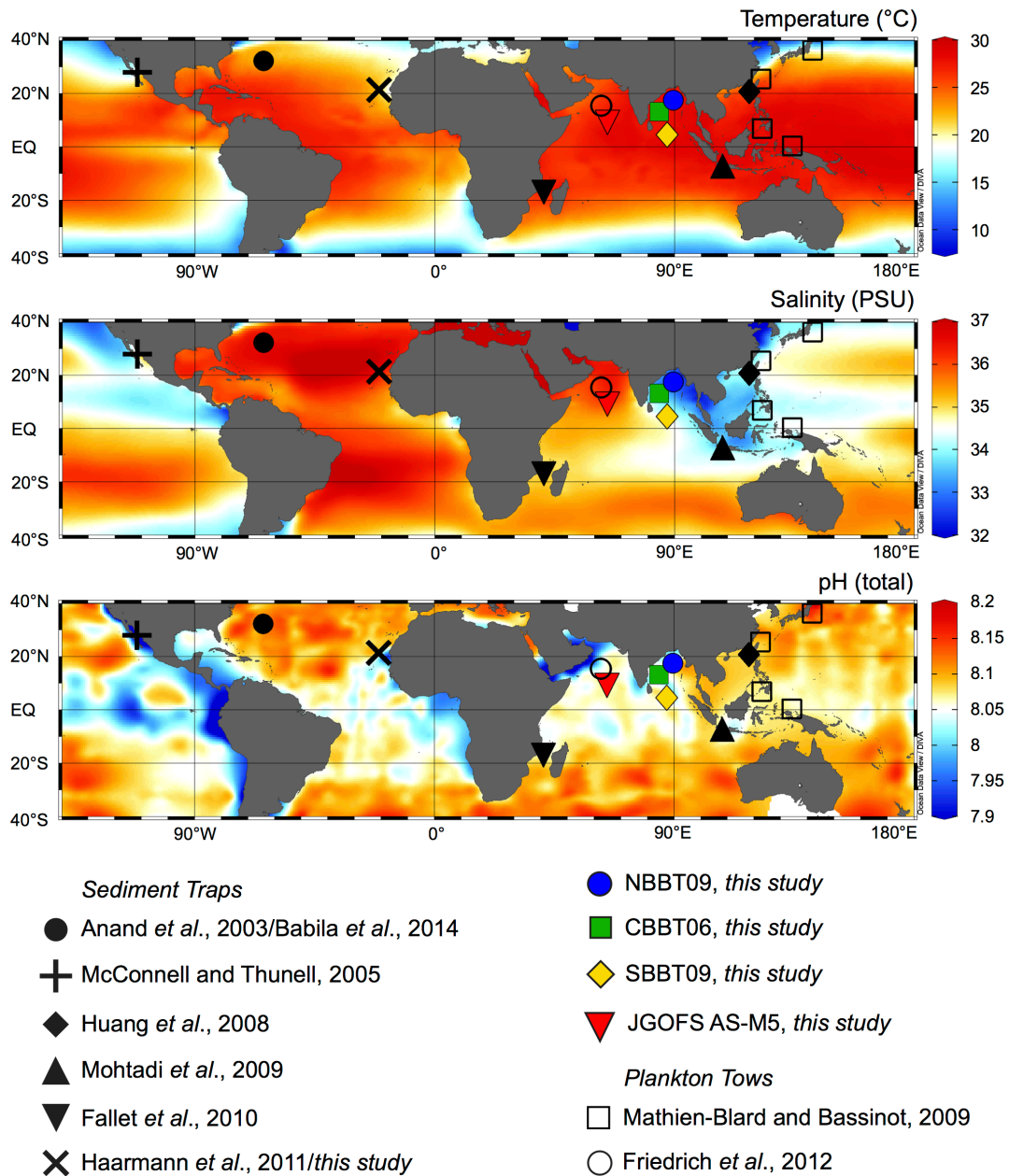
872

873

874

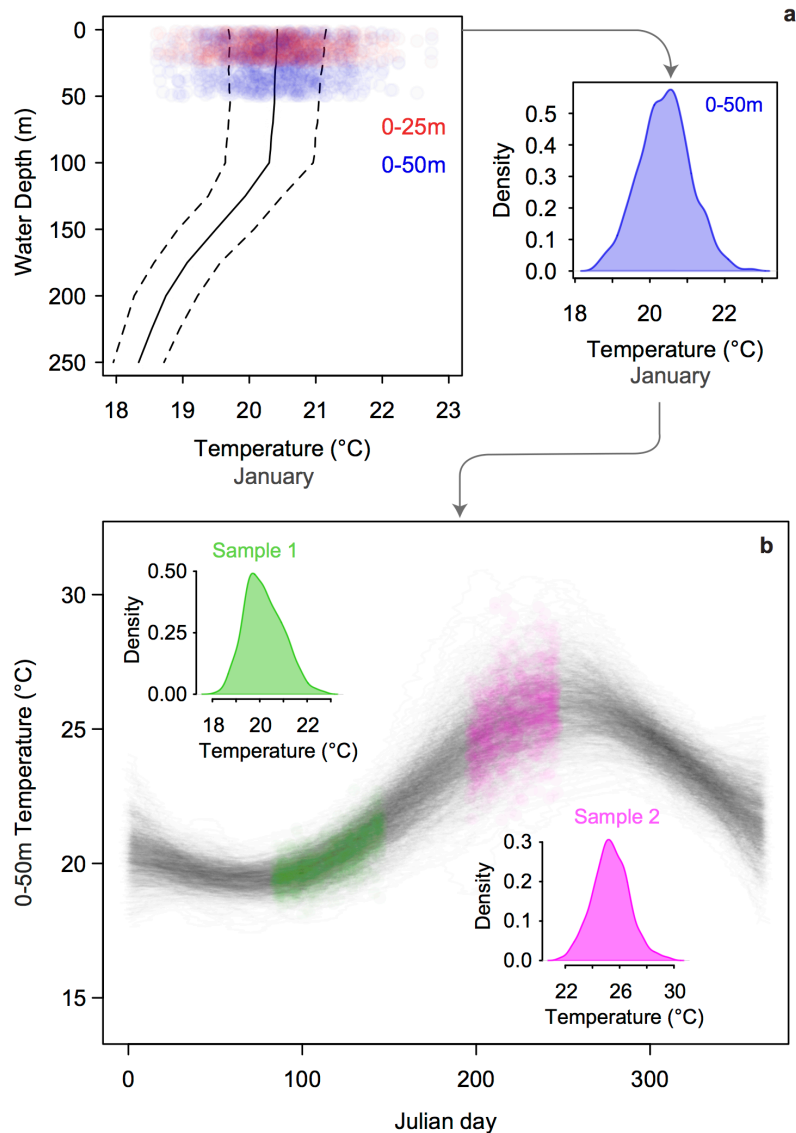
875

876



877

878 **Figure 1** Location of sediment traps (solid symbols) and plankton tows (open symbols) used in this
 879 study, overlaid on mean annual SST and SSS at 25m depth from WOA13 (Boyer *et al.*, 2013), and pH
 880 at 25m depth from GLODAPv2 (Key *et al.*, 2015; Lauvset *et al.*, 2016). Note, the tropical Atlantic trap
 881 site used in this study is located ~120 nm further offshore than that of Haarmann *et al.*, (2011).

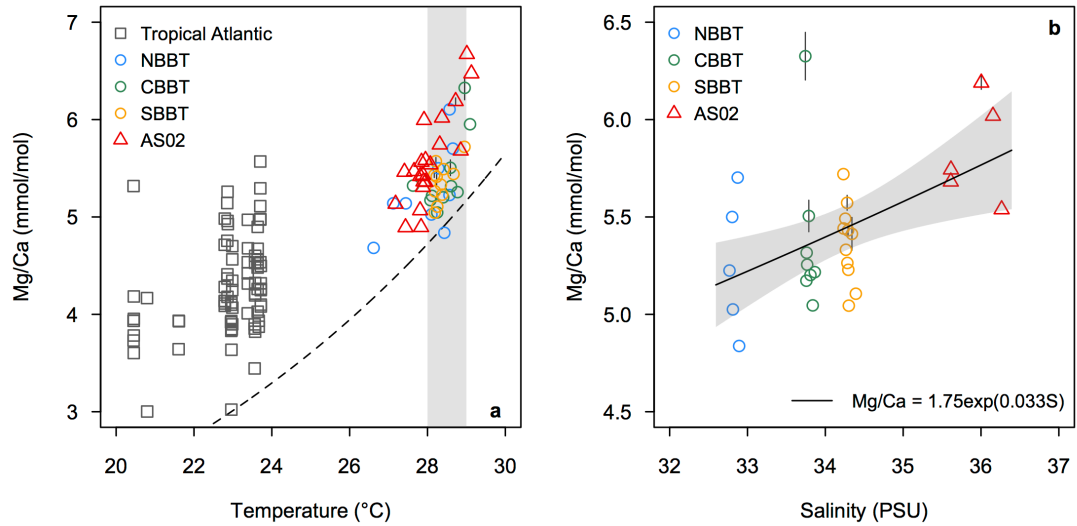


882

883 **Figure 2** Calculation of temperature and salinity for time-period represented by each trap sample at
 884 habitat depth of *G. ruber* (white) using WOA13 monthly climatologies at each trap site and a Monte-
 885 Carlo approach; (a) for each month, a random value is drawn from the population of
 886 temperatures/salinities from within the specified depth habitat range, accounting for the uncertainty
 887 associated with the climatological mean (blue dots = 0-50 m, red dots = 0-25 m) (b) a random sample
 888 is then drawn from these habitat-depth temperature/salinity populations for each month, and the data is
 889 fitted with a GAM (versus Julian day). A day is then randomly drawn from between the open/close
 890 date of each trap sample (after adjustment for sinking and calcification time), and the
 891 temperature/salinity for that day is calculated based on the GAM fit. This process is repeated 10,000
 892 times to fully explore the range in possible calcification temperatures and salinities for each trap
 893 sample, accounting for the depth habitat, error associated with the WOA13 monthly climatologies
 894 (short term and inter-annual variability), and the period of time represented by each trap sample. The
 895 example shown is temperature data for the Sargasso Sea (Anand *et al.*, 2003; Babila *et al.*, 2014). After
 896 first generating monthly carbonate chemistry climatologies for each site (section 2.4), the same process
 897 is used to calculate carbonate chemistry estimates for each trap/tow sample.
 898

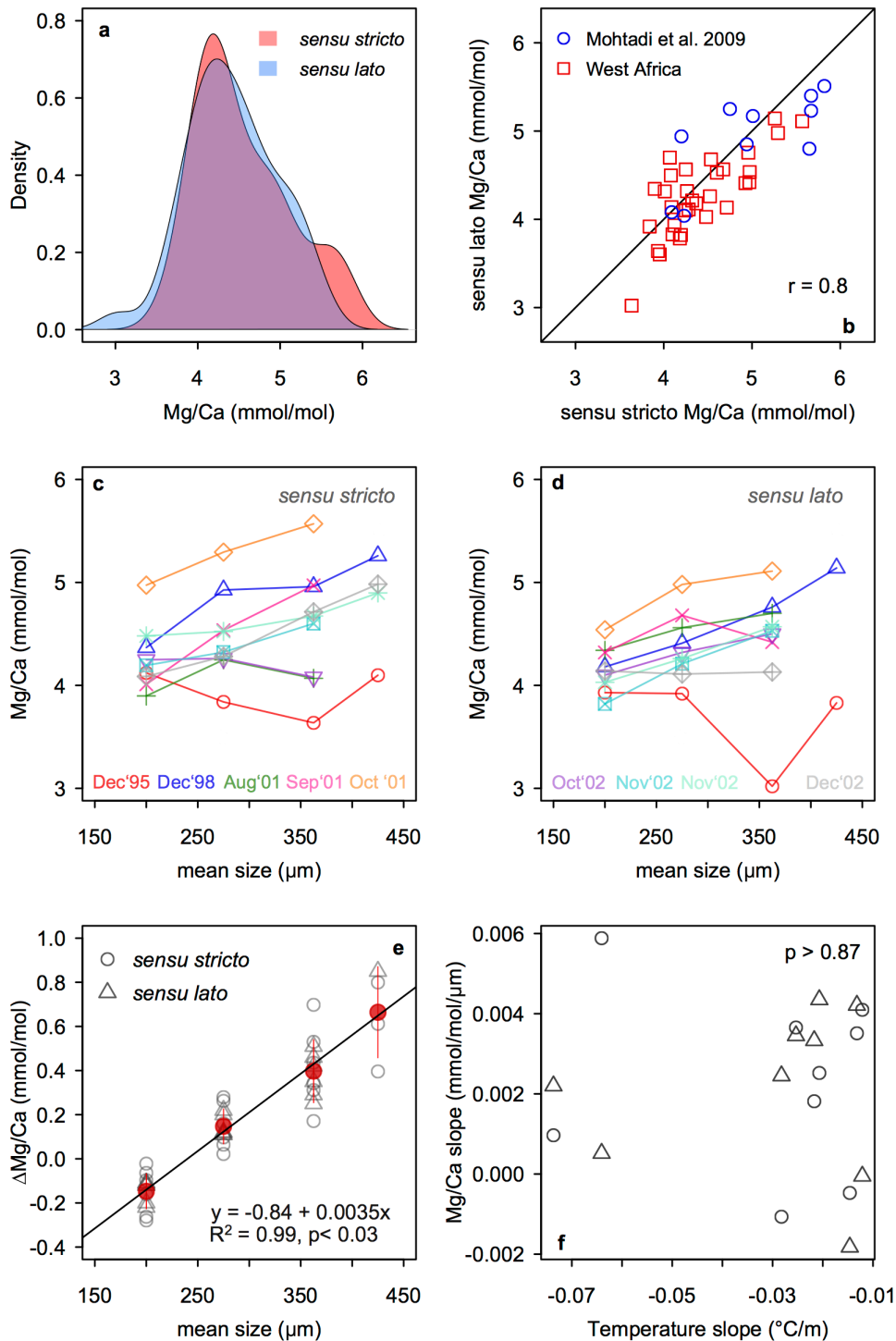
899

900



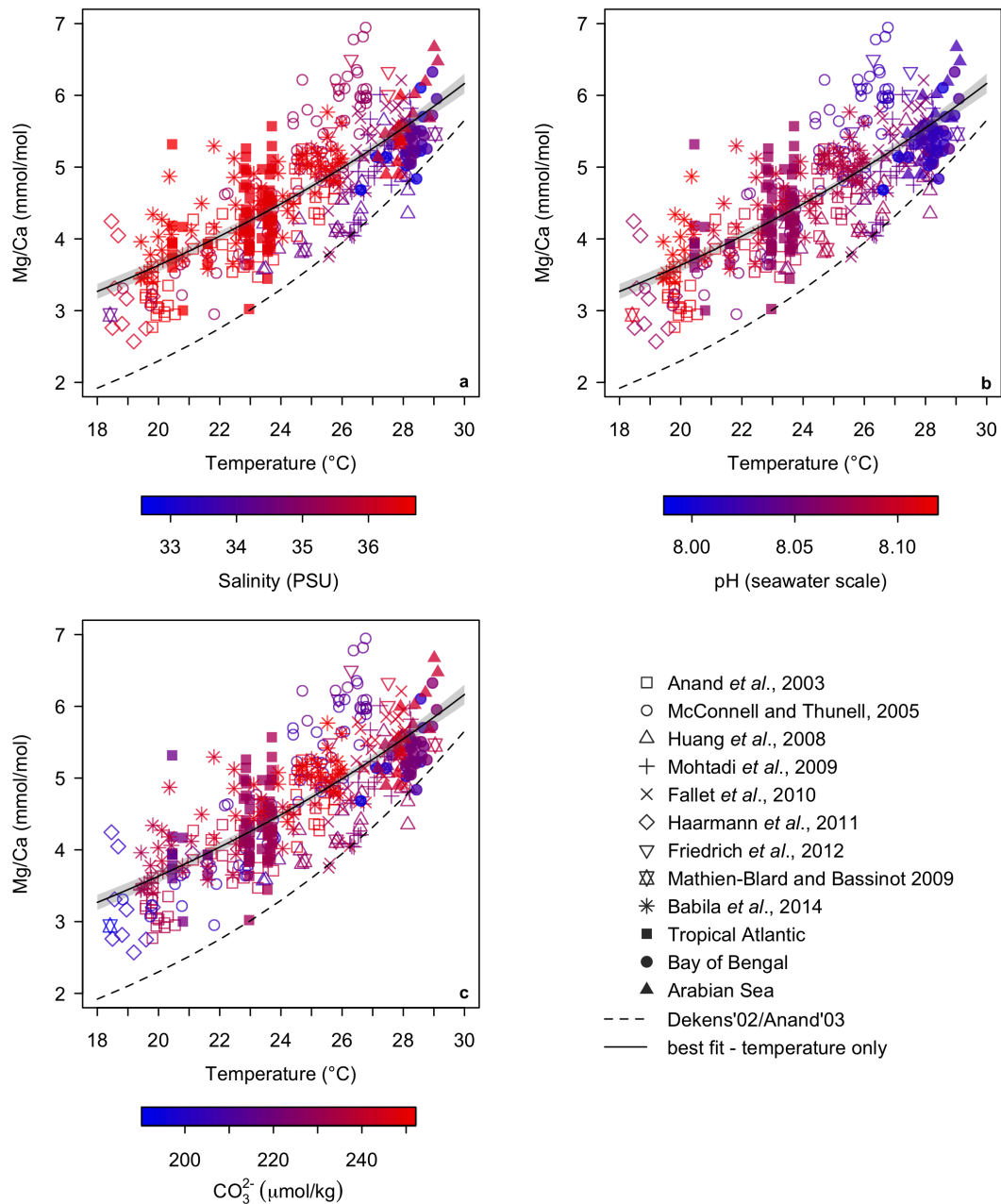
901

902 **Figure 3 (a)** New Mg/Ca data from the Arabian Sea/Bay of Bengal and the tropical Atlantic, analysed
 903 as part of this study, plotted versus climatological temperature (0-50 m, Methods). The calibration of
 904 Dekens *et al.*, (2002)/Anand *et al.*, (2003) is shown by the dashed line. The grey box represents data
 905 between 28 and 29 °C shown in panel b. Error bars are $\pm 1\sigma$ **(b)** Mg/Ca versus salinity in the Arabian
 906 Sea/Bay of Bengal. Only samples with a temperature between 28-29 °C (grey box in a), and a pH of >
 907 8.00 are plotted. The best fit to this subset of data is shown by the solid line, with the 95% confidence
 908 interval shown in grey. The slightly higher spread in the NBBT data is likely due to the fewer number
 909 of individual foraminifera comprising each sample analysed.
 910



911

912 **Figure 4** (a) probability density of Mg/Ca in *G. ruber* (w) *sensu stricto* and *G. ruber* (w) *sensu lato* (all
 913 size fractions) from paired samples (b) Mg/Ca in *G. ruber* (w) *sensu stricto* versus Mg/Ca in *G. ruber*
 914 (w) *sensu lato* in paired samples. There is no significant difference in mean Mg/Ca or variance
 915 between the two morphotypes. Mg/Ca versus mean test size in (c) *G. ruber* (w) *sensu stricto* and (d) *G.*
 916 *ruber* (w) *sensu lato*, with different colors/symbols representing different trap samples (e) Δ Mg/Ca (the
 917 difference relative to the mean Mg/Ca of the 150-250 μ m and 250-300 μ m size fraction for each sample)
 918 plotted against mean test size, excluding the 33% of data that do not show an increasing trend. Red
 919 circles show the mean Δ Mg/Ca of both morphotypes for each size fraction. Error bars are $\pm 1\sigma$ (f) slope
 920 of the temperature change in the upper 50m of water column during the time-period represented by
 921 each sample (Δ Temperature/ Δ depth) versus slope of Mg/Ca-size relationship in each sample
 922 (Δ Mg/Ca/ Δ size) (see SM).



923

924 **Figure 5** Mg/Ca plotted against temperature climatological temperature (0-50 m, Methods) (a) salinity
 925 represented by colour (b) pH represented by colour, and (c) $[\text{CO}_3^{2-}]$ represented by colour. The best fit
 926 (accounting for only temperature) is shown by the solid line (Eq. S1), with the 95% confidence interval
 927 shown in grey. The calibration of Dekens *et al.*, 2002/Anand *et al.*, 2003 ('multi-species') is shown by
 928 the dashed line.

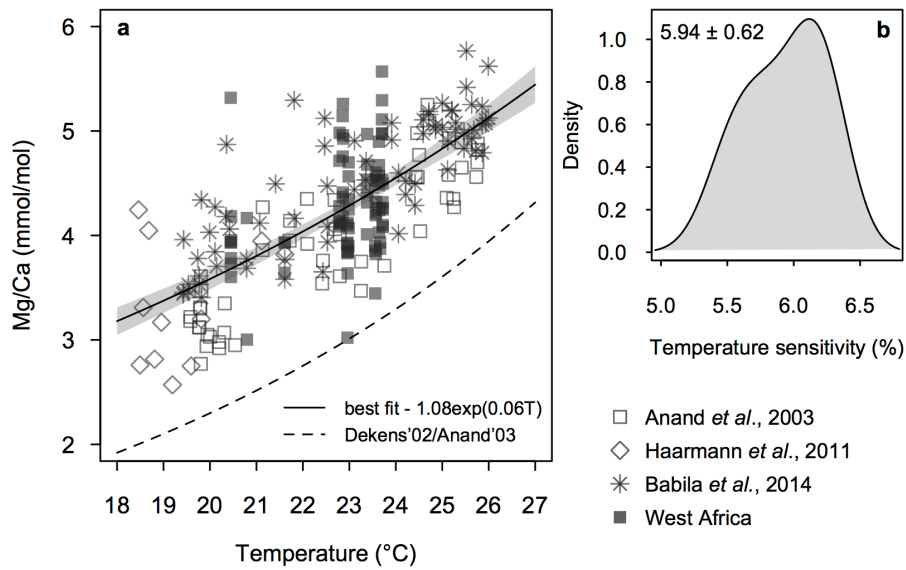
929

930

931

932

933



934
 935 **Figure 6 (a)** Mg/Ca versus climatological temperature (0-50 m, Methods) from a subset of data with a
 936 narrow range in salinity and significantly reduced covariance between temperature and salinity/pH.
 937 The best fit to this subset of data is shown by the solid line, with the 95% confidence interval shown in
 938 grey. The calibration line of Dekens *et al.*, 2002/Anand *et al.*, 2003 is shown by the dashed line. Note
 939 the calibration line of Dekens *et al.*, 2002/Anand *et al.*, 2003 does not fit the data of Anand *et al.*
 940 (2003) when climatological temperature, rather than the $\delta^{18}\text{O}_{\text{calcite}}-\delta^{18}\text{O}_{\text{water}}$ temperature, is used.
 941 Although the ‘multi-species’ equation of Anand *et al.* (2003) is plotted here, the same point stands for
 942 the *G. ruber* (w) calibrations of Anand *et al.* (2003) **(b)** ‘extreme jackknife’ of the dataset; each of the
 943 constituent datasets was successively removed from the subset of data and the temperature regression
 944 was re-run. The results demonstrate that no individual dataset is significantly biasing the results.
 945

946

947

948

949

950

951

952

953

954

955

956

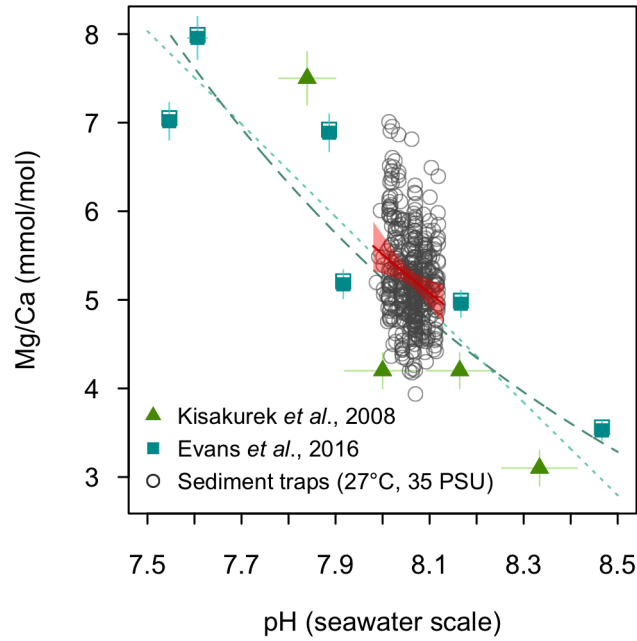
957

958

959

960

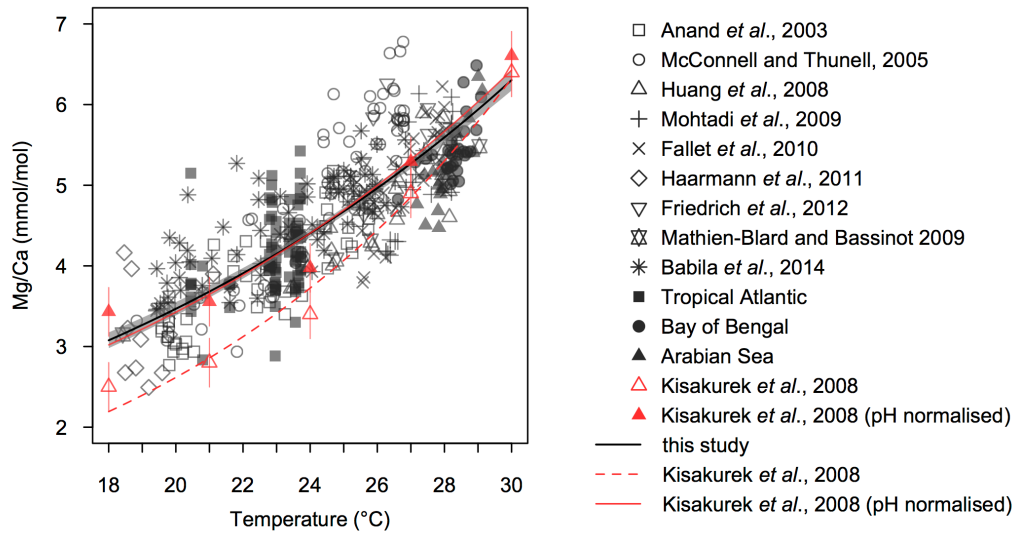
961



962
 963
 964
 965
 966
 967
 968
 969
 970
 971
 972
 973
 974
 975

Figure 7 Mg/Ca versus pH (seawater scale), showing both the sediment trap data from this study (normalised to 27 °C and 35 PSU using a temperature sensitivity of 6.0 %/°C and a salinity sensitivity of 3.3 %/PSU) and the data from the culture studies of Kisakürek *et al.*, (2008)/Evans *et al.*, (2016). The data of Evans *et al.*, (2016) were normalised to 27 °C and 35 PSU using a temperature sensitivity of 6.0 %/°C and a salinity sensitivity of 3.3 %/PSU, and only data from foraminifera cultured at modern seawater Mg/Ca are included. The uncorrected data are shown by the open squares. The data of Kisakürek *et al.*, (2008) were cultured at 27 °C/35 PSU. The best fit to the sediment trap data (exponential) is shown by the solid red line, with the 95% confidence interval shown in red. The best fit to the cultured data is shown by the dashed line (exponential, Eq. S11), and the dotted line (linear). The pH data of Kisakürek *et al.*, (2008)/Evans *et al.*, (2016) were converted to the seawater scale. Error bars are $\pm 1\sigma$.

976
 977
 978
 979
 980
 981
 982
 983
 984
 985
 986
 987



988

989 **Figure 8** Mg/Ca versus temperature, showing both the sediment trap data from this study and cultured
 990 *G. ruber* (white) data of Kisakürek *et al.*, (2008). The sediment trap data are plotted versus
 991 climatological temperature (0-50 m, Methods). The sediment trap data have been normalised to a
 992 salinity of 35 PSU and a pH of 8.05 units using a 3.3%/PSU salinity sensitivity (Eq. 1) and a -8.3%/0.1
 993 pH unit sensitivity (Eq. 3), respectively. The data of Kisakürek *et al.*, (2008) are shown both
 994 uncorrected (open triangles) and corrected (filled triangles) for the effect of pH on Mg/Ca.
 995 The calibration line suggested by this study if pH is the controlling parameter (Eq. 3) is shown by the black
 996 line (for a salinity of 35 PSU and a pH of 8.05 units), with the 95% confidence interval shown in grey.
 997 The dashed red line indicates the best fit to the culture data without correcting for the effect of pH on
 998 Mg/Ca. The solid red line indicates the best fit to the culture data after correction for the effect of pH
 999 on Mg/Ca (the pH data of Kisakürek *et al.*, (2008) were first converted to the seawater scale). Error
 1000 bars are $\pm 1\sigma$.

1001

1002

1003

1004

1005

1006

1007

1008

1009

1010

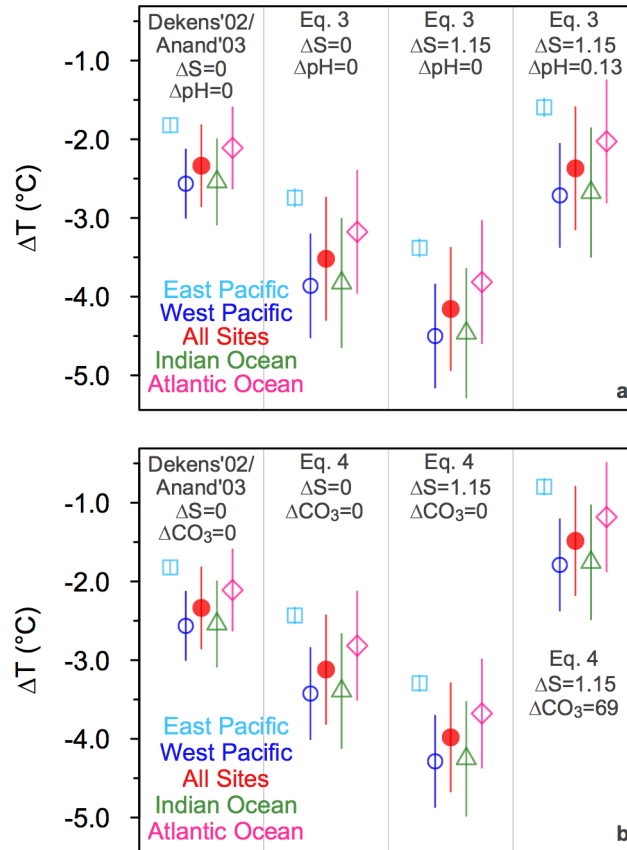
1011

1012

1013

1014

1015



1016

1017 **Figure 9** Magnitude of LGM cooling in the tropical ocean using the calibration of Dekens *et al.*,
 1018 (2002)/Anand *et al.*, (2003) and the calibrations given in this study if (a) pH is the controlling
 1019 carbonates system parameter (Eq. 3) or, (b) $[\text{CO}_3^{2-}]$ is the controlling carbonate system parameter (Eq.
 1020 4). The magnitude of cooling is shown with and without accounting for the whole ocean increase in
 1021 salinity (1.15 units) and pH (0.13 units)/ $[\text{CO}_3^{2-}]$ (69 $\mu\text{mol/kg}$) (supplementary material). Error bars
 1022 ($\pm 1\sigma$) relate only to the standard deviation of the $\Delta\text{Mg/Ca}$ within each region. The true uncertainty of
 1023 the temperature change is dependent on both the uncertainty of the sensitivities of Mg/Ca to T, S, pH
 1024 and/or $[\text{CO}_3^{2-}]$ within the calibration, and the uncertainty in regional changes in salinity, pH/ $[\text{CO}_3^{2-}]$,
 1025 and dissolution during the LGM. Currently, we have very little constraint on regional changes in
 1026 salinity and pH/ $[\text{CO}_3^{2-}]$ during the LGM, thus the uncertainty associated with these changes is
 1027 essentially unquantifiable at present.
 1028